The Journal of Chemical Physics ARTICLE scitation.org/journal/jcp

Rayleigh-Brillouin light scattering spectra of CO_2 from molecular dynamics

Cite as: J. Chem. Phys. 151, 064201 (2019); doi: 10.1063/1.5110676
Submitted: 20 May 2019 • Accepted: 14 June 2019 •
Published Online: 14 August 2019

Seyed Hossein Jamali,[1] Mariette de Groen,[1] Othonas A. Moultos,[1] Remco Hartkamp,[1] Thijs J. H. Vlugt,[1] Wim Ubachs,[2] and Willem van de Water[3,a)]

AFFILIATIONS

[1]Engineering Thermodynamics, Process and Energy Department, Faculty of Mechanical, Maritime and Materials Engineering, Delft University of Technology, Leeghwaterstraat 39, 2628CB Delft, The Netherlands
[2]Department of Physics and Astronomy, LaserLaB, VU University, De Boelelaan 1081, 1081 HV Amsterdam, The Netherlands
[3]Laboratory for Aero and Hydrodynamics, Faculty of Mechanical, Maritime and Materials Engineering, Delft University of Technology, Leeghwaterstraat 29, 2628CB Delft, The Netherlands

[a)]**Electronic mail:** w.vandewater@tudelft.nl

ABSTRACT

Rayleigh-Brillouin light scattering spectra of CO_2 at ultraviolet wavelengths are computed from molecular dynamics which depends on intermolecular potentials only. We find excellent agreement with state of the art experimental data. This agreement was reached in a minimal computational box with sides one scattering wavelength long and integrating the classical trajectories over 20 ns. We also find complete consistency with models based on kinetic theory, which take known values of the transport coefficients as input.

I. INTRODUCTION

The spectrum of scattered light opens a unique window on the transport properties of CO_2. It is determined by density fluctuations at length scales comparable to the scattered light wavelength and time scales in the nanosecond regime. These time scales and length scales have so far been explored incompletely. In this paper, we show for the first time that measured Rayleigh–Brillouin spectra can be reproduced accurately with Molecular Dynamics (MD), using information about intermolecular potentials only. This result opens up new testing grounds for MD and new ways to model the scattering of light off gases that consist of mixtures of polyatomic molecules exploring intramolecular degrees of freedom. While these circumstances are often encountered in applications of practical interest, for example, in laser light scattering off air, devising spectral models for them are very difficult.

In the kinetic regime, when the wavelength of scattered light is smaller than the mean free path between collisions, density fluctuations are described by the Boltzmann equation, which needs information about intermolecular interaction. At the other extreme, with many mean free paths in a scattering wavelength, a continuum approach applies, with fluctuating hydrodynamics that need macroscopic transport coefficients.

Light scattering in this paper is in the kinetic regime. The problem then is the approximation of the Boltzmann collision integral. The successful and now widely used model by Boley *et al.*[1] and Tenti *et al.*[2] uses the Wang Chang-Uhlenbeck eigentheory which takes known values of the transport coefficients as input.[3] For polyatomic gases, a large unknown is the elusive bulk viscosity η_b. The bulk viscosity is associated with the excitation and relaxation of internal molecular degrees of freedom: rotations and vibrations.[4,30] For CO_2, the value needed to explain experimental light scattering spectra appears to be a factor of 10^4 smaller than the experimental value of η_b.[5,6] This dramatic difference is due to the slowness of the relaxation of vibrational modes. At the frequencies associated with light scattering, vibrational modes remain frozen-in. By contrast, at acoustical (megahertz) frequencies, vibrational modes fully participate in the exchange of internal energy, leading to a bulk viscosity that is much larger.

The gigahertz frequencies in light scattering follow from the frequency of sound at wavelengths comparable to that of light. The measurement of η_b at these frequencies is indirect; it follows from

analyzing scattered spectra using models. The standard experimental practice is to select a value of the bulk viscosity, such that the model fits the experimental result best. Of the transport coefficients needed in the spectral model, not only the bulk viscosity is unknown at high frequencies but also the heat conductivity λ_{th} as it is determined by the energy of internal motion. In principle, therefore, spectral models need a best guess of the value of several transport coefficients simultaneously.

Carbon dioxide is a prime greenhouse gas, which has spurred large-scale activity in its capture, transport, and storage.[7–10] In this respect, the confusion about a transport coefficient is unacceptable. Moreover, a better understanding of the transport properties of CO_2 is of relevance for current and future exploration of Mars, with CO_2 the main constituent of its atmosphere.[11]

With the advent of modern laser and optics technology, light scattering spectra can be measured extremely precisely. The question is if these spectra can be reproduced with molecular dynamics simulations. The challenge of MD simulations is the large number of particles needed and the long integration time to reach a statistical accuracy comparable to that of the experiment.

The number of particles follows from the gas density and minimal edge size of the computational box, which should equal the scattering wavelength. The scattering wavenumber k_{sc} is determined by the incident laser wavelength and the scattering angle. With $\lambda_{\text{sc}} = 2\pi/k_{\text{sc}} \approx 2.5 \times 10^{-7}$ m and a pressure of 2 bars, we need approximately one million particles. From the experimental spectra, we learn that frequency resolution should be approximately 0.05 GHz, leading to a minimum simulation time of $t_{\text{sim}} = 2 \times 10^{-8}$ s. In fact, a multiple of this time is needed in order to achieve sufficient statistical accuracy. We will demonstrate that these requirements can actually be met easily.

In a recent paper, Bruno *et al.*[12] successfully compare Rayleigh-Brillouin spectra computed through Monte Carlo simulations of the Boltzmann equation with experimental spectra. However, this comparison is at the expense of adjusted parameters of collision cross sections and rotational relaxation times. Instead, in the present paper, we will do molecular dynamics simulations, using interatomic and intermolecular potentials only. For the first time, we will show that the result of this approach can be compared very well to state of the art experimental spectra. As a test, we simulate an argon scattering spectrum and compare it to a benchmark experiment.

In spectral lineshape models,[1,2] the bulk viscosity is an unknown. Also using MD simulations, we compute this unknown η_{b} and compare it to the value that produces the best agreement between the model spectrum and experiment.

In Sec. II, we will briefly explain how to obtain light scattering spectra from the computed trajectories of molecules in a simulated gas, while the used MD techniques are described in Sec. III. For completeness, a concise description of the experiment is given in Sec. IV. A detailed report of all experimental techniques and procedures is given by Gu *et al.*[13]. In Sec. V A, we will test our procedure to compute a spectrum from molecular dynamics using an experimental spectrum of argon, which we consider as a benchmark spectrum. In Sec. V B, we compare an experimental light scattering spectrum of CO_2 to the result of the molecular dynamics simulation. Finally, in Sec. V C, we will demonstrate the application of spectral models to the experiments, obtaining values of the bulk viscosity from least-squares fits. These numbers are then compared to values obtained from a small MD simulation.

II. LIGHT SCATTERING

The measured spectrum of scattered light is the space-time Fourier transform of microscopic density fluctuations. This time-dependent density field can be constructed from time series of particle coordinates $\boldsymbol{r}_i(t)$ computed by MD,

$$\rho_j(\boldsymbol{r}, t) = \sum_{i=1}^{N_p} \delta(\boldsymbol{r} - \boldsymbol{r}_i(t)),$$

where N_p is the number of particles in the simulation. For CO_2, $\boldsymbol{r}_i$ is the location of the center of mass, that is, the location of the carbon atom. A total of $j = 1, \ldots, N_{\text{r}}$ with $N_{\text{r}} = 100$ independent realizations of a gas was simulated. These realizations were started in parallel on the Intel®Xeon®Processor E5-2697A v4 with 32 cores. After equilibration at the set (experimental) temperature, 10^3 microscopic density fields $\rho(\boldsymbol{x}, t_k)$ were registered from configuration snapshots, lasting $t_{\text{sim}} = 2 \times 10^{-8}$ s for each realization. In this way, the lowest and highest frequencies reachable are $f = 0.05$ GHz and 25 GHz, respectively.

The light scattering spectrum $S(\boldsymbol{k}, \omega)$ is the space-time Fourier transform of the van Hove correlation function,[14]

$$G(\boldsymbol{r}, \tau) = \langle \rho(\boldsymbol{x} + \boldsymbol{r}, \tau + t)\, \rho(\boldsymbol{x}, t) \rangle,$$

with the average $\langle \cdots \rangle$ over time, space and realizations. Through the Wiener-Khintchine theorem, this is the same as the temporal Fourier transform of the intermediate scattering function,

$$F(\boldsymbol{k}, \tau) = \frac{1}{N_p} \left\langle \widetilde{\rho}(\boldsymbol{k}, t + \tau) \widetilde{\rho}^*(\boldsymbol{k}, t) \right\rangle. \tag{1}$$

As integration over long times t_{sim} was expensive, Schoen *et al.*[15] approximated the long-time tails of $F(\boldsymbol{k}, \tau)$ with hydrodynamic-type functions before doing the Fourier transform. With the computational resources at our disposition, this is not strictly necessary. Typically, $F(\boldsymbol{k}, \tau)$ decays in 10^{-9} s, while our integration time is a factor 20 longer.

The light scattering spectrum can be computed directly as the energy spectrum of $\rho(\boldsymbol{r}, t)$, and the route via $F(\boldsymbol{k}, \tau)$ is not necessary. Practically, for each realization j, we store the Fourier transform at discrete times $t = t_k$, $k = 0, \ldots, N_t - 1$,

$$\widetilde{\rho}_j(\boldsymbol{k}, t) = \frac{1}{N_p} \sum_{n=1}^{N_r} \mathrm{e}^{i\boldsymbol{k}\cdot\boldsymbol{r}_n(t)}. \tag{2}$$

Next, we compute the spectrum,

$$S_j(\boldsymbol{k}, \omega) = \left| \frac{1}{N_t} \sum_{k=0}^{N_t} (\widetilde{\rho}_j(\boldsymbol{k}, t_k) - \langle \widetilde{\rho}(\boldsymbol{k}) \rangle)\, H(t_k)\, \mathrm{e}^{-i\omega t_k} \right|^2, \tag{3}$$

with $\langle \widetilde{\rho}(\boldsymbol{k}) \rangle$ being the average over realizations and time of the spatial Fourier transform of the microscopic density and with the filter $H(t) = \sin^2(\pi t / t_{\text{sim}})$ being a cure against spectral leak. The summation in Eq. (3) for discrete ω_k is done via the fast Fourier transform.

The spectra $S_j(\boldsymbol{k}, \omega)$ must be averaged over realizations j and over directions of the wave vector. The length of $\boldsymbol{k}$ is set by the laser wavelength and scattering angle of the experiment. By comparing results to those obtained with reflective boundary conditions, we demonstrate below that the computational box *must be with periodic boundary conditions*.

For periodic boundary conditions, particles that exit the box at, for example, $x = L$, are reinjected at $x = 0$. If L is not a multiple of the scattering wavelength λ_{sc}, this event gives rise to a phase jump $2\pi L/\lambda_{sc}$ in Eq. (2). Also, for periodic boundary conditions, the direction of $\boldsymbol{k}$ *must* be chosen along the coordinate axes. If not, the contribution of the boundary crossing particle experiences a phase jump of $2\pi k_x/k$. Disobeyance of these rules leads to large fluctuations of $S_j(\boldsymbol{k}, \omega)$. Since the effect is associated with boundary crossings, it is in fact a finite-size effect. These restrictions do not apply to the MD simulations with reflective boundaries, where we can check the isotropy of light scattering spectra by varying the direction of $\boldsymbol{k}$.

Finally, the spectra $S_j(\boldsymbol{k}, \omega)$ are averaged over realizations,

$$S(k,\omega) = \frac{1}{N_r}\sum_{j=1}^{N_r}\frac{S_j(\boldsymbol{k},\omega)}{\langle\widetilde{\rho}^2(\boldsymbol{k})\rangle - \langle\widetilde{\rho}(\boldsymbol{k})\rangle^2},$$

where we also averaged over $\boldsymbol{k}$ vectors pointing in the x, y, and z directions. The statistical accuracy of the computed light scattering spectrum depends on the number of realizations N_r. In addition, the Fourier transform in Eq. (3) may be split over half-overlapping sections of the time series with the result averaged. This further improves statistical accuracy, but at the expense of spectral resolution. However, the latter may be prevented by endowing $F(\boldsymbol{k}, \tau)$ with an analytic long-time tail.

III. MOLECULAR DYNAMICS SIMULATIONS

Molecular dynamics views molecules as classical objects, even when they explore internal degrees of freedom, which are of essential quantum nature. Some of these quantum effects emerge in the form of the potentials used. All MD simulations were performed in LAMMPS (version 16 Feb. 2016).[16] The initial configurations of molecules were constructed by using PACKMOL,[17] and input data files for LAMMPS were generated by using VMD.[18] All simulations are performed in a microcanonical ensemble (NVE), where the density and total energy of the system correspond to the temperature (297 K) and pressure specified by the experimental condition.

The force field parameters of argon and CO_2 are obtained from the work of Köster *et al.*[19] and Zhang and Duan.[20] Lennard-Jones interactions are truncated at a cutoff radius of 15 Å. Analytic tail corrections are included for the calculation of energy and pressure. Lorentz–Berthelot mixing rules are applied for dissimilar Lennard–Jones interaction sites.[21] Electrostatic interactions are truncated at a cutoff radius of 15 Å according to the damped shifted force method.[22] CO_2 molecules in the simulations are rigid objects with a bond length of 1.163 Å and an angle of 180°. The equations of motion are integrated with a time step of 10 fs, and the total length of a simulation is 20 ns. In case of the reflective boundary condition, the integration time step was reduced to 2 fs to prevent instabilities. The trajectories of the centers of mass are stored every $t_k = k \times 2 \times 10^{-11}$ s. These snapshots form the microscopic density function $\rho(\boldsymbol{r}, t)$.

In addition, transport coefficients of CO_2 were computed in a simulation box containing 6880 CO_2 molecules with a side-length of 518.796 Å. The Einstein relations are used to obtain the transport properties (shear viscosity, bulk viscosity, and thermal conductivity), and properties of the system are sampled according to the order-n algorithm[23] by using the OCTP plugin for LAMMPS.[24] For computing transport coefficients, the length of each simulation is 200 ns with an integration time step of 1 fs. The statistical uncertainties in the computed transport coefficients are obtained by performing 10 independent simulations.

IV. EXPERIMENTAL SETUP

A schematic view of the setup for the measurement of spontaneous Rayleigh-Brillouin scattering is shown in Fig. 1. The light from a narrowband continuous-wave laser is scattered off a gas contained in a temperature-controlled gas cell, with scattered light collected at an angle of 90°. The laser is a frequency-doubled Ti:Sa laser delivering light at λ = 403 nm, 2 MHz bandwidth, and 400 mW of output power. The enhancement cavity amplifies the circulating power delivering a scattering intensity of 4 Watt in the interaction region.[13]

The scattering angle (90 ± 0.9)° is determined by means of sets of diaphragms and pinholes and checked by using a reference laser beam. The scattered light is filtered by a diaphragm which covers an opening angle of 2°, collected by a set of lenses, further filtered by an extra pinhole (d = 50 μm), and then directed into a hemispherical scanning Fabry–Perot interferometer, which is used to resolve the frequency spectrum of the scattered light. The light is detected using a photomultiplier tube (PMT) which is operated in the photon-counting mode. All measurements are performed at room temperature, 297 ± 1 K.

When comparing computed spectra to experimental results, it is crucial to allow for the instrument function $S(f)$. As a function of frequency f, $S(f)$ is a periodic array of peaks, characterized by

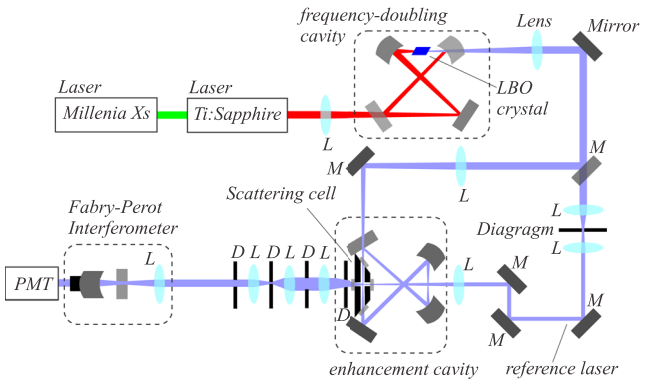

FIG. 1. Schematic diagram of the experimental setup for spontaneous Rayleigh-Brillouin scattering. The laser beam (blue line) is amplified in an enhancement cavity to increase the scattering intensity. Scattered light at an angle of 90° is collimated and directed onto a piezoscannable Fabry–Perot interferometer for spectral analyses and detected on a photomultiplier tube (PMT).

two parameters, the free spectral range f_{FSR}, the period of the peaks, and f_{w}, the width of the peaks. The periodicity owes to the use of a Frabry-Perot spectrometer in the experiment. The instrument function is

$$S(f) = \frac{1}{1 + \left[\frac{2f_{\mathrm{FSR}}}{\pi f_{\mathrm{w}}} \sin\left(\frac{\pi f}{f_{\mathrm{fsr}}}\right)\right]^2}. \tag{4}$$

In the sequel, computed spectra $E(f) = S(k_{\mathrm{sc}}, \omega/2\pi)$ were convolved with this instrument function and normalized such that the integral over one free spectral range is unity.

V. RESULTS

Rayleigh-Brillouin light scattering is characterized by the uniformity parameter y, which is (up to a constant) the ratio of the scattering wavelength over the mean free path between collisions, which is equivalent to $y = p/(k_{\mathrm{sc}} v_0\, \eta_{\mathrm{s}})$, with thermal velocity $v_0 = (2k_{\mathrm{B}}T/m)^{1/2}$, where k_{B} is the Boltzmann constant and m is the (molecular) mass. For the shear viscosity η_{s}, we used the experimental value, that from MD was very close. Our experiments and simulations are in the kinetic regime with $y = \mathcal{O}(1)$.

A. Light scattering spectra of argon

To demonstrate that the kinetics generated by MD correctly produces light scattering spectra, we simulate spectra of a gas whose atoms do not display internal degrees of freedom (at our temperature) and whose interaction potentials are well known.[19]

High precision argon spectra were measured at ultraviolet wavelengths (λ = 403 nm, $k_{\mathrm{sc}} = 2.205 \times 10^7$ m^{-1}).[25] We use these spectra as a benchmark in a comparison with MD calculations. The uniformity parameter is $y = 1.15$. For these experiments, the parameters of the instrument function are $f_{\mathrm{FSR}} = 7.553 \times 10^9$ Hz and $f_{\mathrm{w}} = 1.390 \times 10^8$ Hz.

Molecular dynamics simulations were performed in a cubic box with side length L = 2849.6 Å, temperature T = 297 K, and pressure 2 bars, corresponding to $N_p = 1.13 \times 10^6$ Ar atoms. The simulations were repeated 100 times, each with a different initial configuration and each with a total simulation time of 20 ns.

Figure 2(a) shows a simulated spectrum using periodic boundaries and compare it to the experimental spectrum. Even with the minimal box size with side length λ_{sc}, the agreement with the experiment is excellent. This demonstrates that our choice of the computational box, its boundary conditions, and the used averaging time t_{sim} is adequate. Since periodic boundary conditions impose a restriction on the scattering wave vector $\boldsymbol{k}_{\mathrm{sc}}$, we repeated the simulation using reflective boundary conditions where such a restriction no longer applies. However, Fig. 2(b) demonstrates that the simulated spectrum for the reflective boundary conditions strongly disagrees with the experiment.

At this temperature, the velocity of sound is v_s = 320.2 m/s. Sound with wavelength equal to the scattering wavelength λ_{sc} has frequency $v_s/\lambda_{\mathrm{sc}}$ = 0.98 GHz. This corresponds to the shoulder in the spectrum of Fig. 2(a). In case of the reflective boundary condition, a feature at *half* this frequency can be seen. This corresponds to standing acoustic waves in the computation box with wavelength $\lambda_{\mathrm{sc}}/2$, which is its lowest resonance mode.

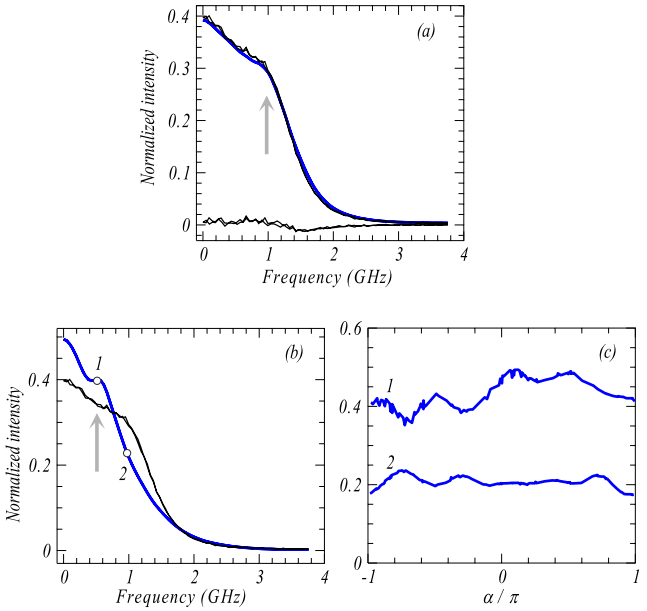

FIG. 2. Measured light scattering spectrum of Ar compared to MD simulations. (a) Using periodic boundary conditions and (b) with reflective boundary conditions. The full black lines are the experimental results, with positive and negative frequencies overlayed. The blue lines are the MD results. The lower black lines are the difference between experiments and MD results. All spectra were normalized to integral $\int E(f)\, df = 1$, where the integration runs over one free spectral range. In (a), the arrow points to the frequency of sound with wavelength equal to the box size, and in (b), the arrow points to the sound frequency with wavelength equal to the twice the box size. Notice that due to the periodic instrument function, the high-frequency tails of the spectra do not return to $E(f) = 0$ exactly. (c) Dependence of the spectrum $S(\boldsymbol{k}_{\mathrm{sc}}, \omega)$ on the angle α with the x-axis of $\boldsymbol{k}_{\mathrm{sc}}$ in the x y-plane. The random vectors were restricted to this plane, $k_{\mathrm{sc}_z}/k_{\mathrm{sc}} < 0.1$. The two curves with 1, 2 correspond to the frequencies indicated in (b).

In a computational box with reflective boundary conditions, there is no restriction on the direction of the scattering wave vector $\boldsymbol{k}_{\mathrm{sc}}$, and the simulated spectrum was averaged over 1024 directions, randomly selected on the sphere. By picking vectors $\boldsymbol{k}_{\mathrm{sc}}$ close to the x y- plane ($k_{\mathrm{sc}_z}/k_{\mathrm{sc}} < 0.1$) and computing the spectrum for each of those, the angular dependence of the spectrum shown in Fig. 2(c) was obtained. It shows preferred directions and is clearly anisotropic, most so at the frequency corresponding to standing waves with wavelength $\lambda_{\mathrm{sc}}/2$.

B. Light scattering spectra of CO_2

Compared to argon, simulating CO_2 spectra is much more challenging because of the much more complex molecular interaction which results in a continuous exchange of rotational and translational energy. The CO_2 spectra, used in a comparison with MD simulations, were obtained by Gu *et al.*[6]. Also these spectra are registered in the ultraviolet, but with experimental conditions slightly different from those of argon. With a laser light wavelength of 366.8 nm, the scattering wavenumber is $k_{\mathrm{sc}} = 2.423 \times 10^7$ m^{-1} (scattering wavelength $\lambda_{\mathrm{sc}} = 2.549 \times 10^{-7}$ m). The uniformity parameter depends on pressure; it is y = 1.6, 2.5, and 3.3 for pressures 2, 3, and 4 bars, respectively. The spectral resolution is slightly less than

that for the experiment performed on Ar, now for CO_2 $f_{FSR} = 7.440 \times 10^9$ Hz and $f_w = 2.32 \times 10^8$ Hz.

Molecular dynamics simulations were done in a minimal box with size $L = 2\pi/k_{sc} = 2593.98$ Å, temperature $T = 297$ K, and number of molecules $N_p = 0.860 \times 10^6$, 1.300×10^6, and 1.740×10^6 for pressures 2, 3, and 4 bars, respectively. Simulations were done for two box sizes. In Figs. 3(a) and 3(b), we compare spectra computed with box side length $L = 2593.98$ Å (a) with one twice as large, containing 8 times more molecules. In both cases, we averaged over $N_r = 100$ realizations. No significant difference between the two box sizes is observed. However, both simulated spectra differ slightly from the experiment. The same type of discrepancy is observed at the larger pressures $p = 3$, 4 bars in Figs. 3(c) and 3(d). In this case, an average over only $N_r = 20$ realizations was done. The convolution of the MD results with the instrument function Eq. (4) smoothes statistical fluctuations of the computed MD spectra. These fluctuations are largest for the smallest pressure.

Despite the more complex intermolecular interaction, the simulated spectra can be compared well to the experiment. We believe that the agreement can be improved by averaging over more simulations N_r. At the lowest pressure $N_r = 100$, but at $p = 3$, and 4 bars, N_r is a mere 20. The statistical accuracy of the experiment increases with pressure; the same behavior was found in the simulation. Merely increasing the number of particles N_p by doubling the side length of the box, as was done in the case of Fig. 3(b), did not improve the statistical accuracy of MD.

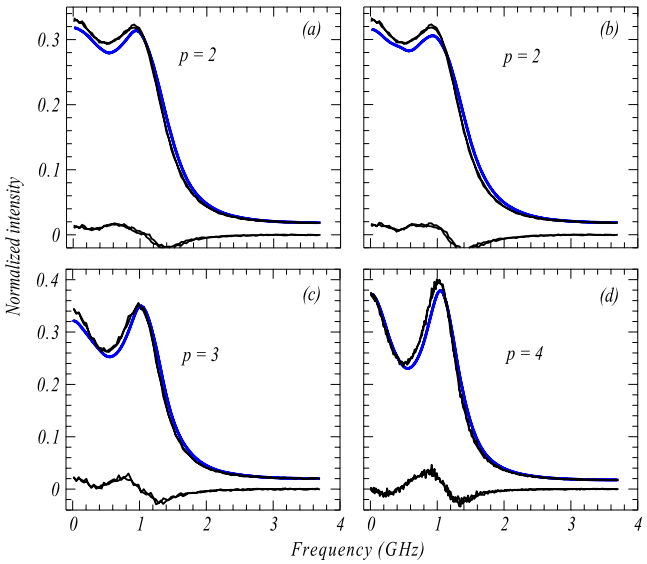

FIG. 3. Measured light scattering spectrum of CO_2 compared to MD simulations. The full black lines are the experimental result, with positive and negative frequencies overlayed. The blue line is the MD results. (a) MD for a box size $L = 2593.98$ Å and (b) for a box size twice as large, $L = 2 \times 2593.98$ Å. The pressure is 2 bars, and averages were taken over $N_r = 100$ realizations. (c) The pressure is 3 bars, $N_r = 20$, (d) $p = 4$ bars, $N_r = 20$. Notice that due to the periodic instrument function, the high-frequency tails of the spectrum do not return to $E(f) = 0$ exactly.

C. Bulk viscosity of CO_2

The kinetic models of Boley *et al.*[1] and Ref. 2 that were introduced in Sec. I can be used as a means to extract the value of transport coefficients from experimental data.[5,6,26,27] The models take these transport coefficients as parameters and can be evaluated extremely quickly as the used eigensystems have only dimension 6 or 7. In fact, this procedure is the only means to obtain a value of the bulk viscosity η_b at the GHz frequencies of light scattering. We will now compare η_b to the one computed from MD.

This procedure is illustrated in Fig. 4 for the 6-mode spectral model[1] and the 7-mode model.[2] These two models differ in the number of eigenmodes used in the approximation of the collision integral[1,2] but should otherwise be comparable. Surprisingly, the 6-mode model approximates the experiment closest, except at $f = 0$. Incidentally, measuring purely elastic spectra ($f = 0$) requires very careful control of unwanted reflections and a completely dust-free cell. The values of η_b, $\eta_b = 5.6 \times 10^{-6}$ kg m^{-1} s^{-1} (6-mode model) and $\eta_b = 6.2 \times 10^{-6}$ kg m^{-1} s^{-1} (7-mode model), were determined in a least-squares fit.

To avoid fitting two unknown transport coefficients to measured spectra, a high-frequency value for λ_{th} was estimated from the Eucken relation, which expresses λ_{th} in the shear viscosity, the diffusivity D, and the heat capacity C_{int} of internal motion,

$$\lambda_{th} = \frac{5}{2}\eta\, C_t + \rho\, D\, C_{int}, \tag{5}$$

with $C_t = 3/2\, R$ being the heat capacity of kinetic motion, $D = 0.57 \times 10^{-5}$m^2 s^{-1} being the self-diffusion coefficient,[28] and R being the gas constant. A high-frequency value of λ_{th} results from allowing for rotations only in C_{int}, which for the linear CO_2 molecule becomes

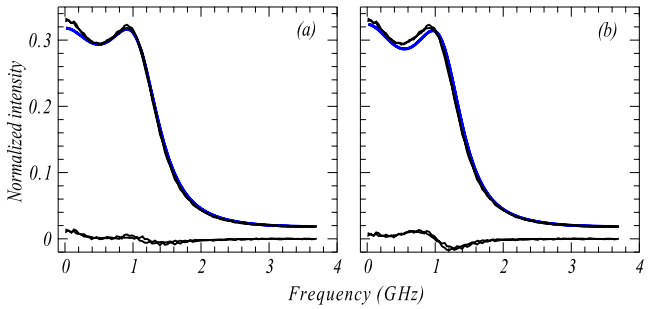

FIG. 4. Measured light scattering spectrum of CO_2 compared to two statistical models. Full (black) lines: experiment and blue lines: model. The lower lines are the difference between the experiment and model. (a) Comparison to the 6-mode model[1] and (b) comparison to the 7-mode model.[2] The experimental conditions are as those of Fig. 3. The models need values of the transport coefficients as input, shear viscosity $\eta = 1.50 \times 10^{-5}$ kg m^{-1} s^{-1} and bulk viscosity $\eta_b = 5.6 \times 10^{-6}$ kg m^{-1} s^{-1} [case (a)], $\eta_b = 6.2 \times 10^{-6}$ kg m^{-1} s^{-1} [case (b)], and heat capacity of internal motion $C_{int} = 2\, R$, for rotations only. For η at 296.6 K, we used the value documented by Boushehri *et al.*,[28] the value of the thermal conductivity was estimated using an Eucken formula,[29] while the values of η_b were determined from a fit of the two models to the experiment in a least-squares procedure. The left ($f < 0$) and right halves of the spectra are shown overlayed. All spectra were normalized to integral $\int E(f)\, df = 1$, where the integration runs over one free spectral range.

$C_{int} = 1\ R$. At temperature $T = 296.55$ K, the low-frequency value is $\lambda_{th} = 1.651 \times 10^{-2}$ W m^{-1} K^{-1},[28] whereas Eq. (5) predicts a high-frequency value $\lambda_{th} = 1.452 \times 10^{-2}$ W m^{-1} K^{-1}. It indeed produces a better fit of the kinetic model, but perhaps accidentally leads to the same estimate of η_b.

Using a small ensemble of CO_2 molecules we computed η_b using the same intermolecular potentials as before. We find $\eta_b = (4.1 \pm 0.7) \times 10^{-6}$ kg m^{-1} s^{-1}, where the uncertainty interval is twice the standard deviation. The MD value of the bulk viscosity can be compared well to the experimental values, $\eta_b = 5.6 \times 10^{-6}$ kg m^{-1} s^{-1} and $\eta_b = 6.2 \times 10^{-6}$ kg m^{-1} s^{-1} for the 6- and 7-mode model, respectively. At high frequencies, kinetic models and MD simulations are consistent, and they both view CO_2 as a rigid object, leading to predictions for light scattering spectra and bulk viscosity that can be compared well.

The result, shown in Fig. 4, demonstrates that MD for scattered light spectra is completely consistent with models based on kinetic theory. Molecular dynamics can directly produce such spectra, circumventing the approximation of the Boltzmann collision integral which is central to these models, but it can also generate the input for those spectral models. On the other hand, MD can simulate spectra for situations where no kinetic theory exists.

VI. CONCLUSION

Through comparison with benchmark experiments, we conclude that a minimal computational box with size equal to the scattering wavelength and periodic boundaries suffices to reproduce Rayleigh Brillouin light scattering spectra. MD simulations can directly express light scattering spectra in parameters of the intermolecular potentials. However, the needed computational resources are large. On the other hand, kinetic models can be evaluated extremely quickly, but at the expense of empirical values for the transport coefficients. We have demonstrated the consistency between these two approaches for CO_2, but at high frequencies. The bulk viscosity of CO_2 dramatically depends on frequency: it drops 4 orders of magnitude between 10^6 and 10^9 Hz. It is not clear how to devise kinetic models for phenomena with variable frequency or multiple time scales. In principle, such frequency dependence can be modeled with MD by allowing for flexible bonds of the CO_2 molecule. Frequency dependence may be explored in light scattering experiments through variation of the scattering angle and thus variation of the scattering wavelength λ_{sc}. Smaller scattering angles correspond to smaller k_{sc}, larger λ_{sc}, and lower frequencies. However, at large λ_{sc}, the number of particles in MD becomes prohibitively large. Obviously, at these wavelengths, scattered light spectra probe the continuum and should be described by statistical hydrodynamics. Molecular dynamics may still play a role by providing the necessary transport coefficients.

ACKNOWLEDGMENTS

This work was sponsored by NWO Exacte Wetenschappen (Physical Sciences) for the use of supercomputer facilities, with financial support from the Nederlandse Organisatie voor Wetenschappelijk Onderzoek (Netherlands Organisation for Scientific Research, NWO). The authors gratefully acknowledge the work of Ziyu Gu, who has obtained the experimental data. The core part of the code that computes the Tenti models has been kindly provided to us by Xingguo Pan. T.J.H.V. acknowledges NWO-CW (Chemical Sciences) for a VICI grant. Othonas A. Moultos gratefully acknowledges the support of NVIDIA Corporation with the donation of the Titan V GPU used for this research.

REFERENCES

[1] C. D. Boley, R. C. Desai, and G. Tenti, "Kinetic models and Brillouin scattering in a molecular gas," Can. J. Phys. **50**, 2158 (1972).
[2] G. Tenti, C. D. Boley, and R. C. Desai, "On the kinetic model description of Rayleigh-Brillouin scattering from molecular gases," Can. J. Phys. **52**, 285 (1974).
[3] C. S. Wang Chang and G. E. Uhlenbeck, Technical Report Research Report No. CM-681, University of Michigan, 1951.
[4] P. Gray and S. A. Rice, "On the kinetic theory of dense liquids. XVIII. The bulk viscosity," J. Chem. Phys. **41**, 3689 (1969).
[5] X. Pan, M. N. Shneider, and R. B. Miles, "Power spectrum of coherent Rayleigh-Brillouin scattering in carbon dioxide," Phys. Rev. A **71**, 045801 (2005).
[6] Z. Gu, W. Ubachs, and W. van de Water, "Rayleigh-Brillouin scatering of carbon dioxide," Opt. Lett. **39**, 3301 (2014).
[7] M. Mikkelsen, M. Jørgensen, and F. C. Krebs, "The teraton challenge. A review of fixation and transformation of carbon dioxide," Energy Environ. Sci. **3**, 43 (2010).
[8] M. E. Boot-Handford, J. C. Abanades, E. J. Anthony, M. J. Blunt, S. Brandani, N. Mac Dowell, J. R. Fernandez, M.-C. Ferrari, R. Gross, J. P. Hallett *et al.*, "Carbon capture and storage update," Energy Environ. Sci. **7**, 130 (2014).
[9] T. Sakakura, J.-C. Choi, and H. Yasuda, "Transformation of carbon dioxide," Chem. Rev. **107**, 2365 (2007).
[10] G. J. van Rooij, H. N. Akse, W. A. Bongers, and M. C. M. van de Sanden, "Plasma for electrification of chemical industry: A case study on CO_2 reduction," Plasma Phys. Controlled Fusion **60**, 014019 (2018).
[11] O. Aharonson, M. T. Zuber, D. E. Smith, G. A. Neumann, W. C. Feldman, and T. H. Prettyman, "Depth, distribution, and density of CO_2 deposition on Mars," J. Geoph. Res. E: Planets **109**, E05004 (2004).
[12] D. Bruno, A. Frezzotti, and G. P. Ghiroldi, "Rayleigh-Brillouin scattering in molecular Oxygen by CT-DSMC simulations," Eur. J. Mech B: Fluids **64**, 8 (2017).
[13] Z. Gu, M. O. Vieitez, E. J. van Duijn, and W. Ubachs, "A Rayleigh-Brillouin scattering spectrometer for ultraviolet wavelengths," Rev. Sci. Instrum. **83**, 053112 (2012).
[14] L. van Hove, "Correlation in space and time and Born approximation scattering in systems of interacting papticles," Phys. Rev. **95**, 249 (1954).
[15] M. Schoen, R. Vogelsang, and C. Hoheisel, "Computation and analysis of the dynamic structure factor $S(k, \omega)$ for small wave vectors," Mol. Phys. **57**, 445 (1986).
[16] S. Plimpton, "Fast parallel algorithms for short-range molecular dynamics," J. Comput. Phys. **117**, 1 (1995). Sandia National Laboratories. LAMMPS Documentation, see https://lammps.sandia.gov/doc/Manual.html.
[17] L. Martínez, R. Andrade, E. G. Birgin, and J. M. Martínez, "PACKMOL: A package for building initial configurations for molecular dynamics simulations," J. Comput. Chem. **30**, 2157 (2009).
[18] W. Humphrey, A. Dalke, and K. Schulten, "VMD: Visual molecular dynamics," J. Mol. Graph. **14**, 33 (1996).
[19] A. Köster, M. Thol, and J. Vrabec, "Molecular models for the hydrogen age: Hydrogen, nitrogen, oxygen, argon, and water," J. Chem. Eng. Data **63**, 305 (2018).
[20] Z. Zhang and Z. Duan, "An optimized molecular potential for carbon dioxide," J. Chem. Phys. **122**, 214507 (2005).

[21]M. P. Allen and D. J. Tildesley, *Computer Simulation of Liquids* (Oxford University Press, Bristol, 1989).
[22]C. J. Fennell and J. D. Gezelter, "Is the Ewald summation still necessary? Pairwise alternatives to the accepted standard for long-range electrostatics," J. Chem. Phys. **124**, 234104 (2006).
[23]D. Dubbeldam, D. C. Ford, D. E. Ellis, and R. Q. Snurr, "A new perspective on the order-*n* algorithm for computing correlation functions," Mol. Simul. **35**, 1084 (2009).
[24]S. H. Jamali, L. Wolff, T. M. Becker, M. de Groen, M. Ramdin, R. Hartkamp, A. Bardow, T. J. H. Vlugt, and O. A. Moultos, "OCTP: A tool for on-the-fly calculation of transport properties of fluids with the order-*n* algorithm in LAMMPS," J. Chem. Inf. Model. **59**, 1290 (2019).
[25]Z. Gu, W. Ubachs, W. Marques, and W. van de Water, "Rayleigh-Brillouin scattering in binary-gas mixtures," Phys. Rev. Lett. **114**, 243902 (2015).
[26]Z. Gu and W. Ubachs, "Temperature-dependent bulk viscosity of nitrogen gas determined from spontaneous Rayleigh-Brillouin scattering," Opt. Lett. **38**, 1110 (2013).
[27]Y. Wang, K. Liang, W. van de Water, W. Marques, and W. Ubachs, "Rayleigh-Brillouin light scattering spectroscopy of nitrous oxide (N_2O)," J. Quant. Spectrosc. Radiat. Transfer **206**, 63 (2018).
[28]A. Boushehri, J. Bzowski, J. Kestin, and E. A. Mason, "Equilibrium and transport properties of eleven polyatomic gases at low density," J. Phys. Chem. Ref. Data **16**, 445 (1987).
[29]A. Chapman and T. G. Cowling, *Mathematical Theory of Non-Uniform Gases*, 3rd ed. (Cambridge Mathematical Library, Cambridge, 1970), ISBN: 052140844.
[30]This is the case for dilute gases, as studied here. In dense monatomic liquids, such as liquid argon, a bulk viscosity is due to two types of collisions: a few hard encounters and multiple soft collisions with many atoms simultaneously.[4]